Drug Design, Development and Therapy

Dovepress
Taylor & Francis Group

Open Access Full Text Article

ORIGINAL RESEARCH

Abnormally Activated MNX1 Promotes Tumor Growth and Osimertinib Resistance and Predicts Survival in EGFR-Mutant Lung Adenocarcinoma

Weiguo Gu[1,*], Jinyu Gan[1,*], Penghui Liu[1], Jianfei Lai[1], Chaoxing Liu[1], Guohua Zhang[2,3], Chao Shi[1], Qingkun Jiang[4], Feng Qiu[1]

[1]Department of Oncology, The First Affiliated Hospital, Jiangxi Medical College, Nanchang University, Nanchang, Jiangxi, People's Republic of China; [2]Department of Oncology, Gaoxin Branch of the First Affiliated Hospital, Jiangxi Medical College, Nanchang University, Nanchang, Jiangxi, People's Republic of China; [3]Nanchang Key Laboratory of Tumor Gene Diagnosis and Innovative Treatment Research, Nanchang, Jiangxi, People's Republic of China; [4]Jiangxi Provincial Key Laboratory of Oral Diseases, Department of Stomatology, The First Affiliated Hospital, Jiangxi Medical College, Nanchang University, Nanchang, Jiangxi, People's Republic of China

*These authors contributed equally to this work

Correspondence: Feng Qiu, Department of Oncology, The First Affiliated Hospital, Jiangxi Medical College, Nanchang University, No. 17 Yong Wai Street, Nanchang, Jiangxi, 330006, People's Republic of China, Email ndyfy01149@ncu.edu.cn; Qingkun Jiang, Jiangxi Provincial Key Laboratory of Oral Diseases, Department of Stomatology, The First Affiliated Hospital, Jiangxi Medical College, Nanchang University, No. 17 Yong Wai Street, Nanchang, Jiangxi, 330006, People's Republic of China, Email ndyfy10001@ncu.edu.cn

Background: Bypass signaling plays an important role in mediating osimertinib resistance in lung adenocarcinoma (LUAD) with epidermal growth factor receptor (EGFR) mutations; however, the role of abnormally activated motor neuron and pancreas homeobox 1 (MNX1) in mediating osimertinib resistance in EGFR-mutant LUAD is unknown.

Methods: Bioinformatics and immunohistochemistry(IHC) analysis identified the MNX1 expression levels in LUAD. The effects of MNX1 and osimertinib on LUAD cell proliferation, invasion, migration, and apoptosis were evaluated using the cell counting kit-8, scratch, EdU, chamber transwell, and flow cytometry assays in vitro. In vivo, the effect of MNX1 expression on tumorigenicity was evaluated using subcutaneous transplanted tumors in nude mice.

Results: Bioinformatics databases and tumor tissue analysis revealed elevated MNX1 expression in LUAD tumor tissues, with high MNX1 expression correlating with poor prognosis. The receiver-operating characteristic(ROC) curve demonstrated that MNX1 has high specificity and sensitivity in diagnosing LUAD from the TCGA dataset. Multivariable COX analysis identified MNX1 as independent prognostic factors for overall survival (OS) in LUAD. Nomogram and calibration plots indicated that combining MNX1 with clinical factors could well predict 1-, 2-, and 3-year OS probabilities in LUAD. Additionally, abnormally activated MNX1 promoted LUAD cell proliferation, invasion, and migration and inhibited apoptosis. MNX1 expression was higher in EGFR-mutant LUAD cells and correlated with osimertinib resistance. The combination of MNX1 depletion and osimertinib suppressed LUAD cell growth and proliferation, inhibited xenograft tumor growth, and reversed osimertinib resistance in vivo. Abnormally activated MNX1 affected PD-L1 expression and induced epithelial-mesenchymal transition (EMT), reversing osimertinib resistance in LUAD cells via the EGFR signaling pathway.

Conclusion: This study demonstrated that abnormally activated MNX1 promoted LUAD cell growth and proliferation and acquired resistance to osimertinib through AKT-mediated EMT and PD-L1. Therefore, MNX1 may be a promising prognostic biomarker and therapeutic target for osimertinib resistance in EGFR-mutant LUAD.

Keywords: lung adenocarcinoma, motor neuron and pancreas homeobox 1, EGFR, osimertinib

Introduction

Lung cancer remains a leading cause of cancer-related mortality, threatening human health worldwide.[1] Osimertinib, a third-generation epidermal growth factor receptor (EGFR) tyrosine kinase inhibitor (EGFR-TKI), can significantly prolong median

Received: 14 May 2025
Accepted: 6 November 2025
Published: 20 December 2025

overall survival (OS) from 12 months to 20–30 months and is a standard first- or further-line treatment for EGFR-mutant advanced non-small cell lung cancer (NSCLC).[2–4] However, most patients experience drug resistance following oral targeted drug therapy, leading to disease progression. Approximately 48–62% of secondary drug resistance to first- and second-generation TKIs is attributed to T790M mutations.[4,5] The EGFR-independent resistance mechanisms are complex and remain controversial. Investigating the specific resistance mechanisms of EGFR-TKIs and identifying novel molecular targets and treatment strategies for EGFR-mutant advanced NSCLC has become a prominent focus of recent research.

Resistance mechanisms of EGFR-TKIs often arise from secondary mutations in the adenosine triphosphate-binding site of EGFR, altering its conformation and preventing effective inhibitor binding, causing drug resistance.[5] Approximately 48–62% of secondary resistance to osimertinib is associated with mutations such as C797S, EGFR L718Q, L844V, G796S/R, and L792F/Y/H et al.[6] However, primary resistance is mainly related to KRAS mutation, BRAF (V600E) mutation, MET or HER2 amplification, and activation of pathways such as HGF/c-MET, RAS-MAPK, and PI3K/AKT.[7–10] Studies have indicated that abnormal activation of cytokines or kinase-activated bypass pathways contributes to osimertinib resistance in EGFR-mutant advanced NSCLC. High interleukin-6 (IL-6) expression in tumor cells correlates with poor prognosis in patients with EGFR-mutant advanced NSCLC treated with EGFR-TKIs.[11] The IL-6 mediated autocrine or paracrine signaling through the IL-6R/JAK1/STAT3 pathway has been implicated in resistance to afatinib and dacomitinib in EGFR (T790M)-mutant NSCLC cells.[12,13] Tian et al reported that osimertinib-resistant cells induce MEK1 and AKT1/2 activation, reducing osimertinib sensitivity through bypass or downstream activation, a key mechanism of drug resistance.[14] Previous studies identified that ID1, a transcription factor, can mediate osimertinib resistance in EGFR T790M-positive NSCLC through abnormal activation and induction of epithelial-mesenchymal transition (EMT).[15] Currently, the molecular mechanisms of bypass pathways leading to osimertinib resistance remain controversial and require further investigation.

Motor neuron and pancreas homeobox 1 (MNX1), a transcription factor primarily located in the nucleus, is vital for motor neuron differentiation and pancreatic β-cell development.[16] Tian et al[17] identified MNX1 as a tumor promoter, with higher expression in breast cancer tissues compared with normal tissues, which is associated with poor prognosis. Pathway enrichment analysis demonstrated that MNX1 regulates nuclear division, cell cycle, and p53 signaling of biological processes. Additionally, MNX1 upregulates c-MYC and CCND1 expression, promoting colorectal cancer (CRC) cell proliferation and distant metastasis through the Wnt/β-catenin signaling pathway.[18] Zhu et al reported that MNX1 transcriptionally suppresses the cycle-dependent kinase $p21^{cip1}$, accelerating cell cycle transition and enhancing cervical cancer proliferation and tumorigenesis in vivo and in vitro.[19] In prostate cancer, MNX1 overexpression upregulates SREBP1 and fatty acid synthetase, potentially promoting lipid synthesis.[20] Additionally, MNX1 acts as an oncogene by transcriptionally activating CCDC34 expression through direct binding to the CCDC34 promoter, thereby promoting the proliferation and growth of lung adenocarcinoma (LUAD) cells.[21]

In this study, we identified MNX1 as an oncogene with significant potential as a diagnostic and prognostic biomarker for LUAD. However, the relationship between MNX1 and osimertinib resistance in LUAD remains unknown. To investigate this, we established osimertinib-sensitive and resistant LUAD cells and observed that MNX1 expression was elevated in osimertinib-resistant cells. Knockdown of MNX1 expression significantly inhibited LUAD cell proliferation and metastasis in vitro and in vivo. Furthermore, MNX1 blockade enhanced the ability of osimertinib to suppress LUAD cell growth and proliferation. Abnormally activated MNX1 affected PD-L1 expression and promoted EMT, contributing to osimertinib resistance in LUAD cells through the EGFR signaling pathway. These findings highlight the importance of elucidating the specific mechanism of osimertinib resistance and exploring new molecular markers and effective therapeutic strategies for patients with EGFR-mutant advanced LUAD.

Materials and Methods

Differentially Expressed Gene Datasets and Microarray Data Information

Gene expression matrix and clinical information were obtained from the Gene Expression Omnibus (GEO, http://www.ncbi.nlm.nih.gov/geo/) and the Cancer Genome Atlas (TCGA, https://portal.gdc.cancer.gov/) databases. GSE180347, from the GPL29738 platform, included 53 NC (PD-L1 negative and TIL negative), 26 PH (PD-L1 positive and TIL positive), 58 NH (PD-L1 negative and TIL positive), and 7 PC (PD-L1 positive and TIL negative) tumor tissue samples

from LUAD, analyzed by immunohistochemistry (IHC). GSE140797, from the GPL13497 platform, included seven LUAD tumor tissues and seven paracancerous tissues. GSE193258, from the GPL20301 platform, included four EGFR-mutant LUAD cell lines (H2935, H827, H1975, and PC-9), all treated with osimertinib.

Analysis of Differentially Expressed Genes (DEGs) by Datasets in LUAD

The gene expression matrix of microarray data and DEGs were analyzed using R software. The DEGs were selected based on the criteria: $|\log_2 FC| > 1$ and P-value < 0.05. Heatmaps and volcano plots were generated for the selected DEGs. The biological functions of DEGs in LUAD were analyzed using the Kyoto encyclopedia of genes and genomes (KEGG) and gene ontology (GO), followed by pathway enrichment analysis with R software to identify pathways associated with the target gene and assess their significance.[21] The GO analysis included cellular components(CC), biological processes(BP), and molecular functions(MF).[22] Venn diagrams (https://bioinfogp.cnb.csic.es/tools/venny/) were used to overlap DEGs across GSE180347, GSE193258, and GSE140797. Kaplan–Meier Plots were generated using the GEPIA2 database (http://gepia2.cancer-pku.cn/), and clinicopathological information and gene expression data were downloaded from the TCGA database. Data analysis was standardized using R packages, and receiver-operating characteristic (ROC) curves were plotted to assess the specificity and sensitivity of DEGs in diagnosing LUAD. The TIMER2 database (http://timer.cistrome.org/) was used to examine gene expression in tumor and normal tissues across multiple cancers.

Analysis of Clinicopathological Information and Construction and Validation of the MNX1-Related Prognostic Model

Univariate and multivariate COX analyses were performed to identify significant prognostic factors associated with OS in LUAD using TCGA datasets, and these factors were used to create a forest plot. A predictive nomogram was generated using the "rms" package in R through multivariate COX analysis. Patients from TCGA datasets were divided into training and validation cohorts in a 2:1 ratio using the R package. Calibration graphs for 1-, 2-, and 3-year survival outcomes were generated to compare the OS predictions from the nomogram with actual survival outcomes.[22]

Cell Lines

Human LUAD cell lines, including H1975, H1650, H827, PC-9, A549, H3255, H520, osimertinib-resistant PC-9 cells (PC9-OR), and H1975 cells (H1975-OR) were obtained from the First Affiliated Hospital of Nanchang University Cancer Center. Osimertinib-resistant cells were continuously cultured at a low concentration (0.1 μmol/L). The human immortalized lung epithelial cell line (BEAS-2B) was obtained from the Department of Burns, First Affiliated Hospital of Nanchang University. Cells were grown in RPMI-1640 and DMEM media (Solarbio, China) supplemented with 10% fetal bovine serum (FBS) at 37 °C in a humidified environment with 5% CO_2.

RNA Extraction and Reverse Transcriptase-Polymerase Chain Reaction (RT-PCR)

Total RNA was isolated from LUAD tissues and cells using TRIzol (Invitrogen, USA) following the manufacturer's instructions. Cells were homogenized to enhance extraction efficiency. RNA was transcribed into cDNA using the HiScript II Q RT SuperMix reagent Kit (Vazyme, Nanjing, China). The SYBR Green PCR Master Mix (Vazyme, Nanjing, China) was used for RT-PCR, and quantitative analysis was performed with the ABI 7500 QPCR System (Applied Biosystems, USA), following the manufacturer's instructions. Relative gene expression was calculated using the $2^{-\Delta\Delta Ct}$ method with GAPDH as internal references for mRNA. TurboFect transfection reagents (Invitrogen, USA) were used to transfect LUAD cells following the manufacturer's protocol. The primer sequences are listed in Table 1.

Cell Proliferation Assay

For the cell proliferation assay and determination of osimertinib of half-maximal inhibitory concentration (IC_{50}), 1×10^3 and 5×10^3 transfected cells were seeded into 96-well plates and incubated for the cell counting kit-8 (CCK-8) assay. The CCK-8 reagent (Bioss, China) was carefully added to each well, and cell growth was monitored at 0, 1, 2, 3, and 4 days. Absorbance at 450 nm was measured using a microplate reader (Thermo Fisher Scientific, USA).

Table 1 The Relative Primer Sequences

Genes	Forward Primer (5′ to 3′)	Reverse Primer (5′ to 3′)
MNX1	GACCCAGGTGAAGATTTGGTTCCAG	GCCCTTCTGTTTCTCCGCTTCC
CX3CL1	TGGGCGTCCTTATCACTCCTGTC	TGGAGGCTCTGGTAGGTGAACATG
CLEC7A	GGTTCTTTCCAGCCCTTGTCCTC	TTAGAGCCCAGTTGCCAGCATTG
SELPLG	ACTCCTCCTGTTGCTGATCCTACTG	CCCAAGGCTTTCTCGGCTTCATC
SPP1	CAGCCGTGGGAAGGACAGTTATG	TCACATCGGAATGCTCATTGCTCTC
IRF8	ACTGCTGGCTGCGTGAATGAAG	GTAATCGTCCACAGAAGGCTCCTTG
NT5E	GCTCCTCTCAATCATGCCGCTTTAG	TTCATCCGTGTGTCTCAGGTTGTTG
CD53	CCTGCTGCTGATTATCCTCCTTGC	ACGCTGCCTTGGTGCTATTGTC
GAPDH	GGAGCGAGATCCCTCCAAAAT	GGCTGTTGTCATACTTCTCATGG
MNX1-homo-1888	GCGGAAACCCACAGUGUUATT	UAACACUGUGGGUUUCCGCTT
MNX1-homo-1074	GCACCAGUUCAAGCUCAACTT	GUUGAGCUUGAACUGGUGCTT
MNX1-homo-1181	GGAUGAAAUGGAAACGCAGTT	CUGCGUUUCCAUUUCAUCCTT

Additionally, cell proliferation was assessed using the EdU Cell Proliferation Kit (BBI Life Sciences Corporation, Shanghai, China). Here, 1×10^4 transfected cells were seeded into 96-well plates for 24 h, mounted in standard mounting media, and imaged using confocal microscopy (Leica, Germany).

Immunohistochemistry

The expression of MNX1, Ki-67, PD-L1, E-cadherin, N-cadherin, and vimentin in paraffin-embedded tissues from patients with NSCLC and xenografted tumors was assessed by IHC at our cancer pathology center. Antigen retrieval was conducted in a water bath using EDTA retrieval buffer (pH 9, 100 mL, Zhongshan Jinqiao Company, Beijing, China). Slides were coated with 50 μL of primary antibody and kept in a 4 °C refrigerator overnight. Horseradish peroxidase-labeled mouse/rabbit universal secondary antibody (Dako and Roche, Switzerland) was added and incubated at 37 °C for 15 min. Diaminobenzidine (DAB, Dako, Carpinteria, CA, USA) was used as the chromogen to visualize immunoreactivity. Histological examinations were conducted independently by two expert pathologists in a double-blinded manner, with appropriate positive and negative controls. Evaluations were based on the criteria of the NSCLC Working Group and the German immunohistochemical semiquantitation scoring standard.

Plasmid Construction and Cell Transfection

Small interfering RNA (siRNA) targeting MNX1 (MNX1 siRNA-1/2/3) was obtained from GenePharma (Shanghai, China). The MNX1 siRNA sequences are provided in Table 1. TurboFect transfection reagent (Invitrogen, USA) was used to transfect H1975, PC-9, PC9-OR, and H1975-OR cells following the manufacturer's protocol. The expression levels of MNXI were detected using RT-PCR and Western blot assays.

Wound Healing Assay

A total of 2×10^5 cells were seeded into 6-well plates and transfected with the siMNX1 plasmid (24 h) or osimertinib (48 h). Once the cells reached 90% confluency, a scratch was made at the bottom of each well using a sterilized 200 μL pipette. The cells were rinsed thrice with phosphate-buffered saline (PBS) and incubated in a fresh medium containing 2% serum at 37 °C in a 5% CO_2 environment. Cell mobility was assessed by measuring the scratch width under a microscope (Leica, Germany) at 0, 24, and 48 h marks.

Transwell Cell Migration and Invasion Assay

The migration and invasion abilities of transfected cells were assessed using Transwell chambers with 24-well plates and 8 μm membrane, with or without 50 μL matrigel. After transfection with siMNX1 (24 h) or osimertinib (48 h), LUAD cells (5×10^4) were suspended in 200 μL of serum-free medium and placed in the upper chamber of the transwell, while 600 μL of medium

containing 10% FBS was added to the lower chamber. After incubation for 24 or 48 h, the cells were scraped, stained, and examined under an optical microscope. The invasion ability was quantified by counting invasive cells in four random fields.

Flow Cytometric Analysis

Apoptosis analysis was conducted using the TransDetect Annexin V-FITC/propidium iodide (PI) cell apoptosis detection kit (TransGen, Beijing, China) and flow cytometry. The LUAD cells were seeded into 6-well plates and transfected with siMNX1 or osimertinib plasmid at 50% confluency for 24 or 48 h. Following transfection, the cells were treated with trypsin and rinsed twice with PBS at 1500 rpm for 5 min. A total of 2 to 8×10^5 cells were collected, and 100 μL binding buffer, 5 μL Annexin V-FITC, and 5 μL PI were added. The mixture was incubated for 15 min, and flow cytometry was performed within 1 h. The apoptosis rate was evaluated, and the percentage of cells at various stages was calculated using flow cytometry software (version 7.6; BD, USA).

Immunofluorescence

Cells (1×10^4) were seeded into 24-well plates, fixed with 4% paraformaldehyde for 15 min, and washed thrice with PBS. Then, 0.1% triton-X100 was applied to promote transparency, followed by blocking with 5% BSA in PBS for 30 min and incubation overnight at 4 °C with the primary antibody (MNX1, ab92606, Abcam, USA) diluted in BSA. The fluorochrome-conjugated secondary antibody (Alexa Fluor 488 Affineur Goat Anti-mouse IgG, Sharp) was added and incubated at 37 °C for 30 min. The cell nuclei were stained with DAPI. Fluorescence was analyzed and visualized using a laser scanning confocal microscope (Leica, Germany).

Protein Extraction and Western Blot Analysis

Proteins were extracted from LUAD cell lines or tissues lysed in lysis buffer (RIPA, Solarbio, Beijing, China) on ice. The proteins were separated using 6–12% SDS-PAGE and blotted onto PVDF membranes by wet electroblotting at a constant current of 200 mA. The primary antibodies used included polyclonal rabbit AKT (ab179463, Abcam, USA), polyclonal rabbit phosphorylated (P)-AKT1/2/3 (Ser473, Affinity Biosciences, Jiang Su, China), MNX1 (ab92606, Abcam, USA), PD-L1 (ab205921, Abcam, USA), MMP9 (ab7603, Abcam, USA), GAPDH (Proteintech, Wuhan, China), N-cadherin (22018-1-AP, Proteintech, China), E-cadherin (60335-1-Ig, Proteintech, China), vimentin (60330-1-Ig, Proteintech, China), and Ki-67 (TA500265, ZSGB-BIO, China).

Xenografted Tumor Model in vivo

To evaluate the effects of MNX1 on tumor growth in vivo, 4–6 week-old mice were obtained from Hunan SJA Laboratory Animal Co., Ltd. (Hunan, China) and randomly (using a computer random number generator) and a single - blind design divided into four groups of five mice each to establish a nude mouse xenograft model. The PC-9 cells (8×10^6), transfected with lentivirus encoding LV-shMNX1 or LV-shNC, were subcutaneously injected into the mice. Tumor volume was measured every three days using calipers and calculated with the formula $0.52 \times L \times W^2$, where L is the tumor length, and W is its width. Osimertinib was administered when the tumor volume reached 50 or 100 mm^3. Tumors were harvested after 47 days when their volumes reached approximately 2000 mm^3. All experiments involving mice were approved and supervised by the Institutional Animal Care and Use Committee of the First Affiliated Hospital of Nanchang University (Nanchang, China).

Statistical Analysis

The experiments were repeated thrice, the bootstrap or permutation test for experiments with $n<5$. The results are presented as mean ± standard deviation (SD). Differences between two samples were assessed using Student's *t*-test, while Fisher's exact test, Spearman correlation, or the chi-squared test, was used to analyze differences in proportion. Univariate and multivariate COX analyses were performed to identify independent prognostic factors, reporting hazard ratio (HR), and 95% confidence interval (CI). Survival rates were analyzed using the Kaplan–Meier method. Statistical and power analysis to justify sample sizes were performed using the Statistical Package for the Social Sciences (version

26.0; SPSS Inc., Chicago, IL, USA), GraphPad Prism (version 9.0; Inc., La Jolla, CA, USA), or R statistical (version 4.0.0; http://www.R-project.org) software. A *P*-value of less than 0.05 was considered statistically significant.

Results

Differentially Expressed Gene Datasets and Microarray Data Information in LUAD

The mRNA expression levels were analyzed using the microarray expression profiling dataset GSE140797 to examine the correlation between DEGs and tumor tissue in LUAD. Seven tumor and paracancerous tissues samples from patients with LUAD were downloaded from the GEO database. The DEGs ($|\log_2 FC| > 1$, *P*-value < 0.05) were analyzed using R packages, revealing 1089 downregulated and 1229 upregulated genes between LUAD tumor and paracancerous tissues. The mRNA expression levels were visualized using a volcano plot (Figure 1A) and heatmap (Figure 1B). Additionally, the Venn diagram presented 44 overlapping genes between GSE140797 and GSE180347 (Figure 1C).

Bioinformatics analysis identified that the mRNA levels of CX3CL1, CLEC7A, SELPLG, MNX1, SPP1, NT5E, CD53, and IRF8 were associated with prognosis in patients with LUAD. The GEPIA2 database demonstrated that high CX3CL1, CLEC7A, and IRF8 expressions were associated with improved OS *(P* < 0.05), whereas high MNX1, SPP1, and NT5E expressions were associated with poor OS *(P* < 0.05) (Figure 1D). In the TCGA dataset, the ROC curve analysis revealed that the expression of eight genes exhibited high specificity and sensitivity for diagnosing LUAD (Figure 1E). Furthermore, CX3CL1, CLEC7A, IRF8, SELPLG, and CD53 expressions were higher in normal tissues compared with LUAD tumor tissues, while MNX1, SPP1, and NT5E expressions were lower in normal tissues (Figure 1F).

Besides, RT-PCR analysis displayed that MNX1 expression was higher in LUAD cells compared with BEAS-2B cells and in EGFR mutant LUAD cells compared with EGFR wildtype A549 cells (Figure 2A–H). The TIMER2 database analysis indicated that MNX1 is highly expressed in most malignant tumors, suggesting it may act as a key oncogene in LUAD (Figure 2I). These findings highlight that MNX1 is an important transcription factor and a potential biomarker in LUAD.

Univariate and Multivariate COX Analyses of MNX1 Prognostic Values in LUAD

Previous our study in bioinformatics analysis indicated that MNX1 as an important oncogene in LUAD. To further investigate its relationship with LUAD, we analyzed LUAD data from the TCGA database. Univariate COX analysis indicated that T, N, M, and pathologic stages, residual tumor, MNX1, and primary therapy outcome were associated with OS in patients with LUAD ($P < 0.1$) (Figure 3A). Multivariable COX analysis revealed that T stages, residual tumor, MNX1, and primary therapy outcome were independent prognostic factors for OS ($P < 0.05$) (Figure 3B and Table 2).

The TCGA dataset was randomly divided into training and validation cohorts at a 2:1 ratio using the R package. A predictive nomogram was generated through multivariate COX analysis. Four variables, including the T stages, residual tumor, MNX1, and primary therapy outcome ($P < 0.05$), were incorporated into the nomogram. The nomogram demonstrated that these factors significantly impacted OS in patients with LUAD (Figure 3C). Calibration plots illustrated that the 1-, 2-, and 3-year OS probabilities predicted by the nomogram closely matched the observed values in patients with LUAD (Figure 3D). Therefore, we suggest that MNX1 is an important diagnostic and prognostic biomarker for LUAD.

MNX1 Was Highly Expressed in LUAD Tumor Tissues and Cell Lines

We observed that MNX1 is associated with poor prognosis and serves as a valuable diagnostic marker for LUAD. To further investigate the role of MNX1 expression in LUAD, six pairs of postoperative LUAD tumor and paracancerous tissues were collected. Western blot and RT-PCR analyses revealed significantly higher levels of MNX1 mRNA and protein in tumor tissues than in paracancerous tissues (Figure 4A and B). Immunohistochemical staining results revealed that MNX1 was mainly localized in the nucleus and cytoplasm, with significantly higher expression in LUAD tumor tissue compared with paracancerous tissues (Figure 4C). Western blot analysis also demonstrated that MNX1 protein expression was higher in EGFR mutant LUAD cells (PC-9, H1975, H1299, and H827) compared with EGFR wildtype cells (A549) and BEAS-2B (Figure 4D). To assess the effect of MNX1 expression on the biological behavior of LUAD cells, we constructed three MNX1 knockdown sequences (siMNX1-1/2/3) and transfected them into LUAD cells (H1975 and PC-9) using turbofect reagent. Western blot and RT-PCR assays confirmed that si-RNA significantly inhibited MNX1

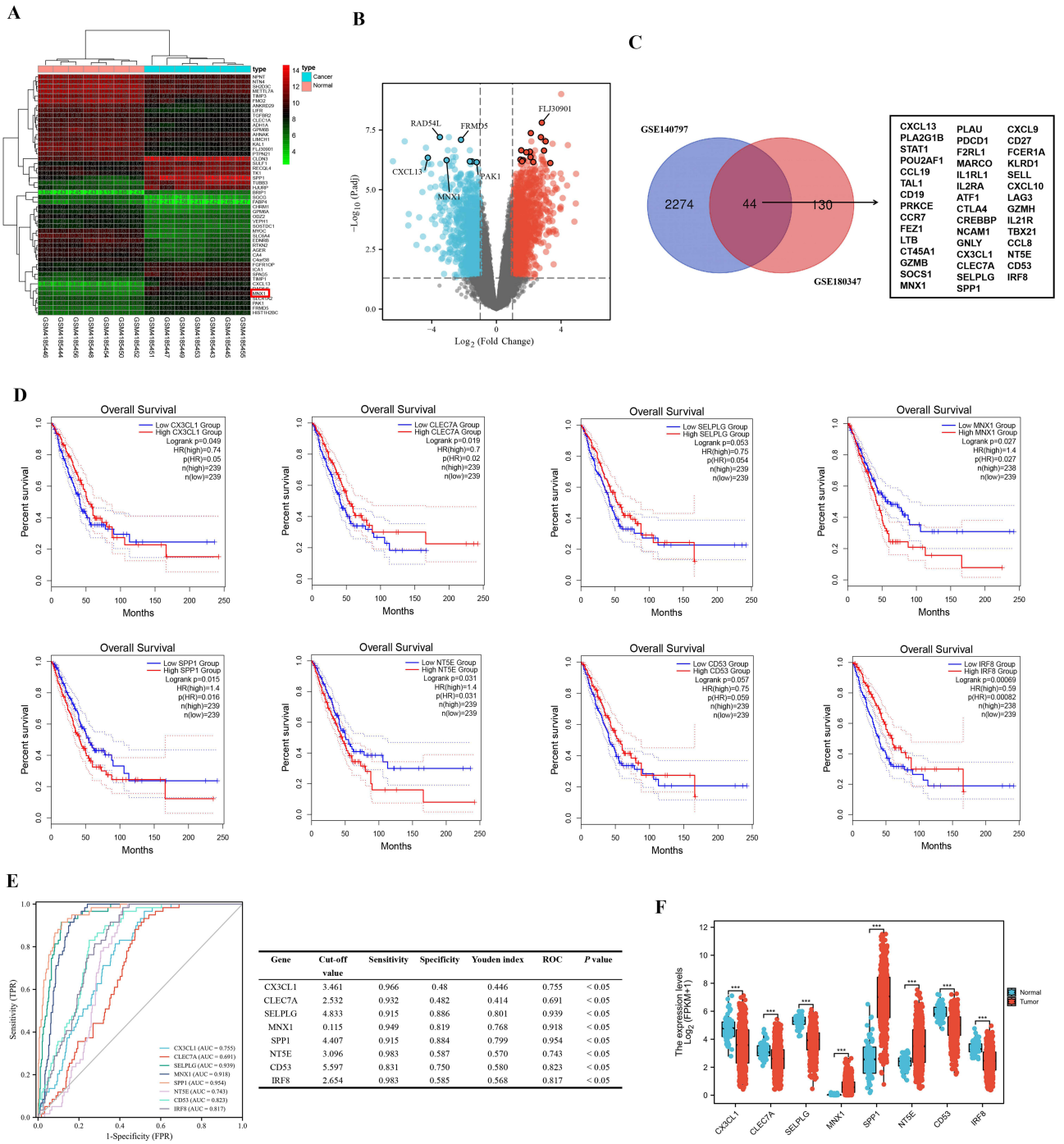

Gene	Cut-off value	Sensitivity	Specificity	Youden index	ROC	*P* value
CX3CL1	3.461	0.966	0.48	0.446	0.755	< 0.05
CLEC7A	2.532	0.932	0.482	0.414	0.691	< 0.05
SELPLG	4.833	0.915	0.886	0.801	0.939	< 0.05
MNX1	0.115	0.949	0.819	0.768	0.918	< 0.05
SPP1	4.407	0.915	0.884	0.799	0.954	< 0.05
NT5E	3.096	0.983	0.587	0.570	0.743	< 0.05
CD53	5.597	0.831	0.750	0.580	0.823	< 0.05
IRF8	2.654	0.983	0.585	0.568	0.817	< 0.05

Figure 1 Differentially expressed gene datasets and microarray data in LUAD. DEGs were selected based on fold change and *P*-value ($|\log_2 FC| > 1$, *P*-value < 0.05) from the mRNA expression profiling dataset GSE140797. Gene expression levels are plotted using a (**A**) heatmap and (**B**) volcano plot for tumor and paracancerous tissues in LUAD. (**C**) Venn diagram illustrates the overlap of 44 genes between the two datasets (GSE140797 and GSE180347). (**D**) OS analysis of CX3CL1, CLEC7A, SELPLG, MNX1, SPP1, NT5E, CD53, and IRF8 based on median values was conducted using Kaplan–Meier survival curves from the GEPIA 2 database. (**E**) ROC curve analysis indicates the high specificity and sensitivity of the eight genes in diagnosing LUAD from the TCGA dataset. (**F**) The histogram indicates differential expression of these eight genes in LUAD tumor and paracancerous tissues from the TCGA database. In the volcano plot, red indicates upregulated genes, and blue indicates downregulated genes; in the heatmap, red represents high expression, black represents moderate expression, and green represents low expression. ***$P < 0.001$.

Abbreviations: LUAD, lung adenocarcinoma; DEGs, differentially expressed genes.

https://doi.org/10.2147/DDDT.S535214

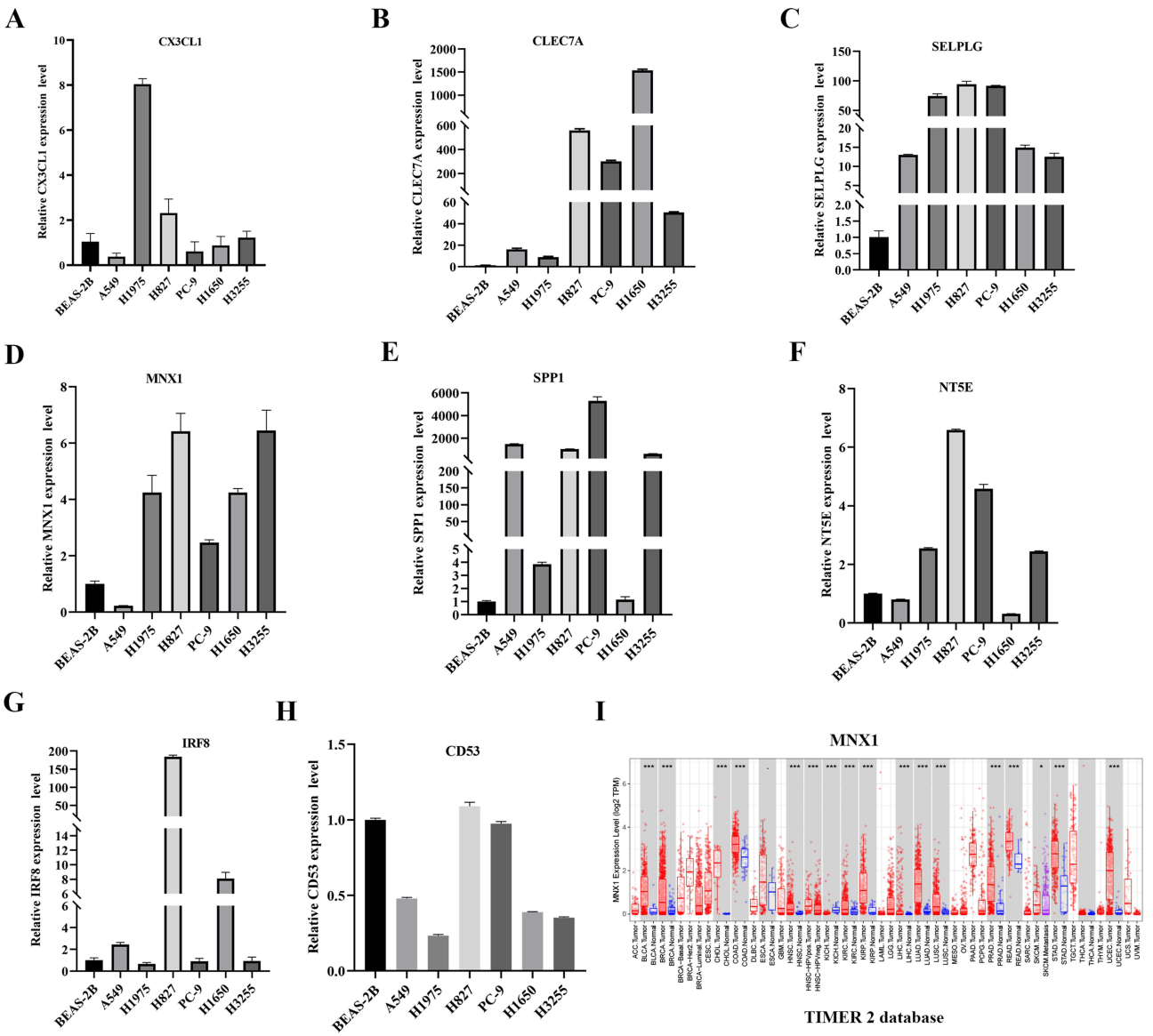

Figure 2 Differentially expressed mRNA in LUAD cells using RT-PCR assay. RT-PCR was performed to assess CX3CL1 (**A**) CLEC7A (**B**) SELPLG (**C**) MNX1 (**D**) SPP1 (**E**) NT5E (**F**) IRF8 (**G**) and CD53 (**H**) expression in LUAD cells and the BEAS-2B. (**I**) TIMER2 database indicates that MNX1 is expressed in most malignant tumors and may act as a key oncogene in LUAD. BEAS-2B, human immortalized lung epithelial cell line. $^{*}P < 0.05$, $^{***}P < 0.001$.

expression levels in LUAD cells (Figure 4E and F). These findings suggest that MNX1 is highly expressed in LUAD cells and tumor tissues, correlates with poor prognosis, and is identified as a key mRNA biomarker.

MNX1 Positively Regulated Tumor Growth and Metastasis in LUAD Cells in vitro

The effects of MNX1 expression on cell proliferation, migration, and invasion were evaluated using cell-based assays. Wound healing, CCK-8, and EdU assays demonstrated that suppressing MNX1 expression significantly inhibited the proliferation of PC-9 and H1975 cells (Figure 5A–C). Transwell assays revealed that MNX1 expression knockdown significantly inhibited the migration and invasion capabilities of PC-9 and H1975 cells (Figure 5D). Flow cytometric analysis revealed that MNX1 expression knockdown significantly increased the apoptosis rate of LUAD cells (Figure 5E). Immunofluorescence assays indicated that MNX1 is mainly localized in the nucleus, and its downregulation significantly reduced nucleus fluorescent brightness in LUAD cells (Figure 5F).

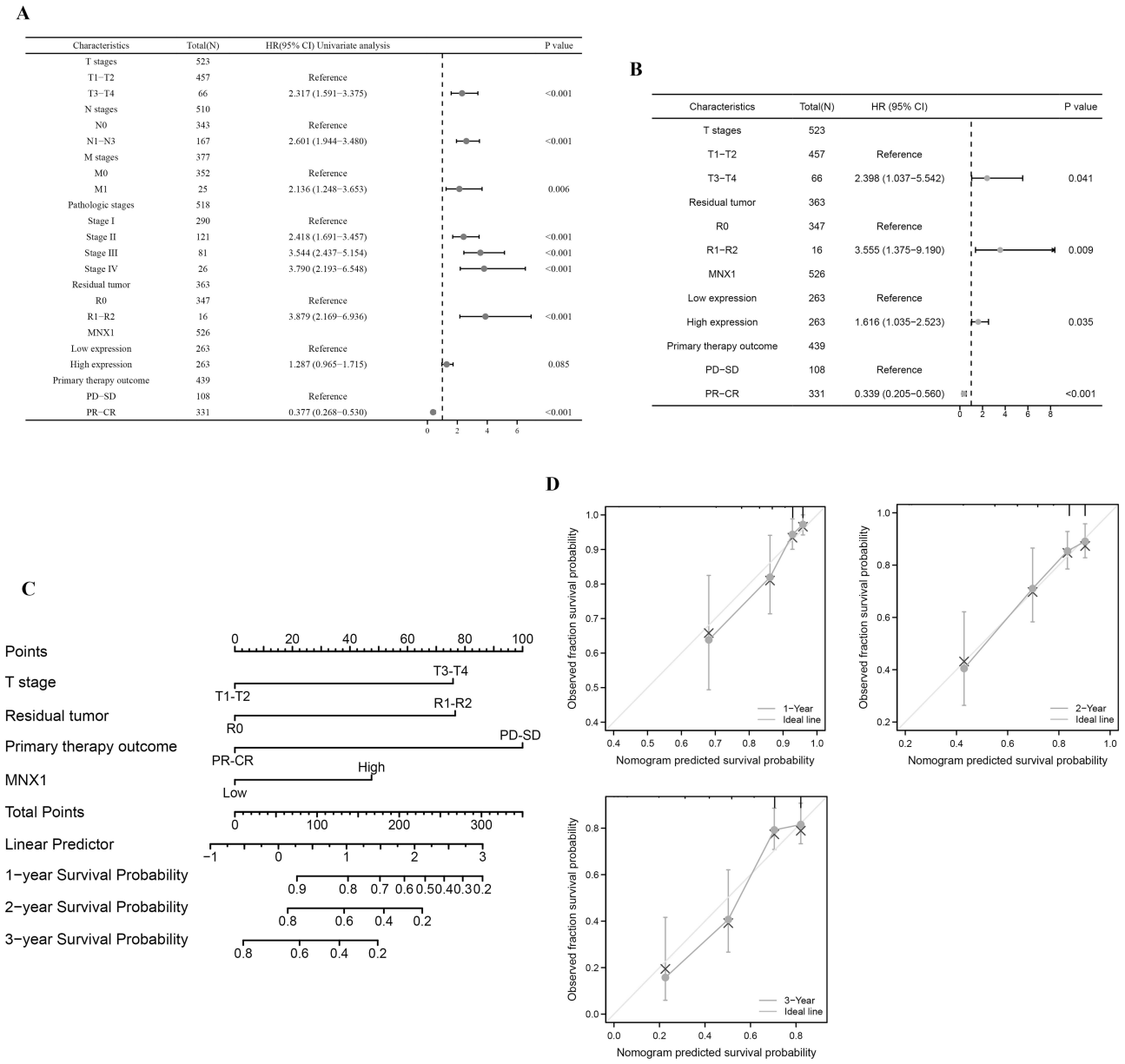

Figure 3 MNX1 is a key diagnostic and prognostic biomarker for LUAD in the TCGA database. (**A**) Univariate and (**B**) multivariate COX analyses of prognostic values in patients with LUAD, presented as forest plots from the TCGA database. Nomogram and calibration plots predict and validate survival outcomes for patients with LUAD in the TCGA database; nomogram predicts 1-, 2-, or 3-year median survival outcomes for patients with LUAD (**C**). Calibration charts of the nomogram assess the predicted versus actual observed OS at 1, 2, and 3 years (**D**).

MNX1 Acquired Resistance to First-Line Osimertinib in Advanced EGFR-Mutant NSCLC

Previous in vitro assays indicated that MNX1 was highly expressed in EGFR-mutant LUAD cells. To further analyze the relationship between TKIs and MNX1, four LUAD cells (H2935, H827, H1975, and PC-9) were treated with osimertinib, and mRNA expression levels were examined using the microarray expression profiling dataset GSE193258 from the GEO database. A Venn diagram revealed an overlap of three DEGs between GSE193258, GSE140797, and GSE180347, with MNX1 expressed in all three datasets (Figure 6A). MNX1 expression was lower in osimertinib-treated groups than untreated groups in EGFR-mutant LUAD cells (H2935, H1975, and PC-9) (Figure 6B). Moreover, 65 paraffin-embedded tissues from advanced EGFR-mutant NSCLC were analyzed, including serum indicators and clinicopathological characteristics (Table 3). The IHC revealed higher MNX1 expression in the resistant group than in the sensitive group (Figure 6C). High MNX1 expression was associated with worse mPFS (23.8 versus 11.3 months, $P < 0.05$, Figure 6D) and OS (39.7 versus 22.8 months, $P < 0.05$, Figure 6E).

https://doi.org/10.2147/DDDT.S535214

Table 2 Univariate and Multivariate Analysis of Relationship Between MNX1 and LUAD From TCGA Database

Characteristics	Groups	Total(N)	Univariate Analysis		Multivariate Analysis	
			HR (95% CI)	*P* value	Hazard Ratio (95% CI)	*P* value
Gender	Female	280	Reference			
	Male	246	1.070 (0.803–1.426)	0.642		
Age	≤65	255	Reference			
	>65	261	1.223 (0.916–1.635)	0.172		
T stages	T1-T2	457	Reference		Reference	
	T3-T4	66	2.317 (1.591–3.375)	<0.001	2.398 (1.037–5.542)	0.041
N stages	N0	343	Reference		Reference	
	N1-N3	167	2.601 (1.944–3.480)	<0.001	2.384 (0.982–5.790)	0.055
M stages	M0	352	Reference		Reference	
	M1	25	2.136 (1.248–3.653)	0.006	1.542 (0.491–4.847)	0.459
Pathologic stages	Stage I	290	Reference		Reference	
	Stage II	121	2.418 (1.691–3.457)	<0.001	0.581 (0.221–1.526)	0.270
	Stage III	81	3.544 (2.437–5.154)	<0.001	0.891 (0.276–2.874)	0.847
	Stage IV	26	3.790 (2.193–6.548)	<0.001		
Residual tumor	R0	347	Reference		Reference	
	R1-R2	16	3.879 (2.169–6.936)	<0.001	3.555 (1.375–9.190)	0.009
MNX1	Low	263	Reference		Reference	
	High	263	1.287 (0.965–1.715)	0.085	1.616 (1.035–2.523)	0.035
Primary therapy outcome	PD-SD	108	Reference		Reference	
	PR-CR	331	0.377 (0.268–0.530)	<0.001	0.339 (0.205–0.560)	<0.001
CD274	Low	263	Reference			
	High	263	1.127 (0.846–1.501)	0.414		

Abbreviations: MNX1, motor neuron and pancreas homeobox 1; CR, Complete Response; PR, Partial Response; SD, Stable Disease; PD, Progressive Disease; CD274, PD-L1.

Osimertinib-sensitive (PC-9 and H1975) and resistant (PC9-OR and H1975-OR) LUAD cells were cultured and constructed, with osimertinib-resistant cells continuously cultured at low concentrations (0.1 μmol/L). The CCK-8 assays revealed that the IC_{50} values of PC9-OR (5.8 versus 0.0206 μmol) and H1975-OR (11.09 versus 0.0101 μmol) were higher than those of PC-9 and H1975 (Figure 6F), indicating that osimertinib-resistant cells required higher osimertinib concentrations. Western blot and RT-PCR analyses demonstrated that MNX1 was overexpressed in PC9-OR and H1975-OR than in PC-9 and H1975 (Figure 6G and H). Furthermore, LUAD cells co-cultured with siMNX1 and osimertinib revealed that MNX1 expression knockdown significantly promoted the LUAD cell resistance to osimertinib through CCK-8 assays (Figure 6I and J). These findings suggest that MNX1 may be associated with osimertinib resistance in EGFR-mutant LUAD cells.

MNX1 Blockade Potentiated Osimertinib to Suppress LUAD Cell Growth and Proliferation

The effects of MNX1 expression and osimertinib on LUAD cell growth and proliferation were evaluated through in vitro assays. The LUAD cells were co-cultured with siMNX1 and osimertinib. The results demonstrated that the combination of osimertinib and siMNX1 significantly suppressed the proliferation, migration, and invasion abilities of PC-9 and H1975 cells (Figure 7A–E). Furthermore, flow cytometric assays revealed that the combination treatment significantly increased the apoptosis rate of LUAD cells than the siMNX1, osimertinib, and control groups (Figure 7F).

Abnormally Activated MNX1 Affected PD-L1 Expression and Promoted EMT to Reverse Osimertinib Resistance in LUAD Cells by EGFR Signaling Pathway

To investigate the molecular mechanism of MNX1 in osimertinib resistance in LUAD, DEGs in patients with LUAD and cells were analyzed using the GSE140797 and GSE193258 datasets. Pathway enrichment analyses through KEGG/GO and GSEA

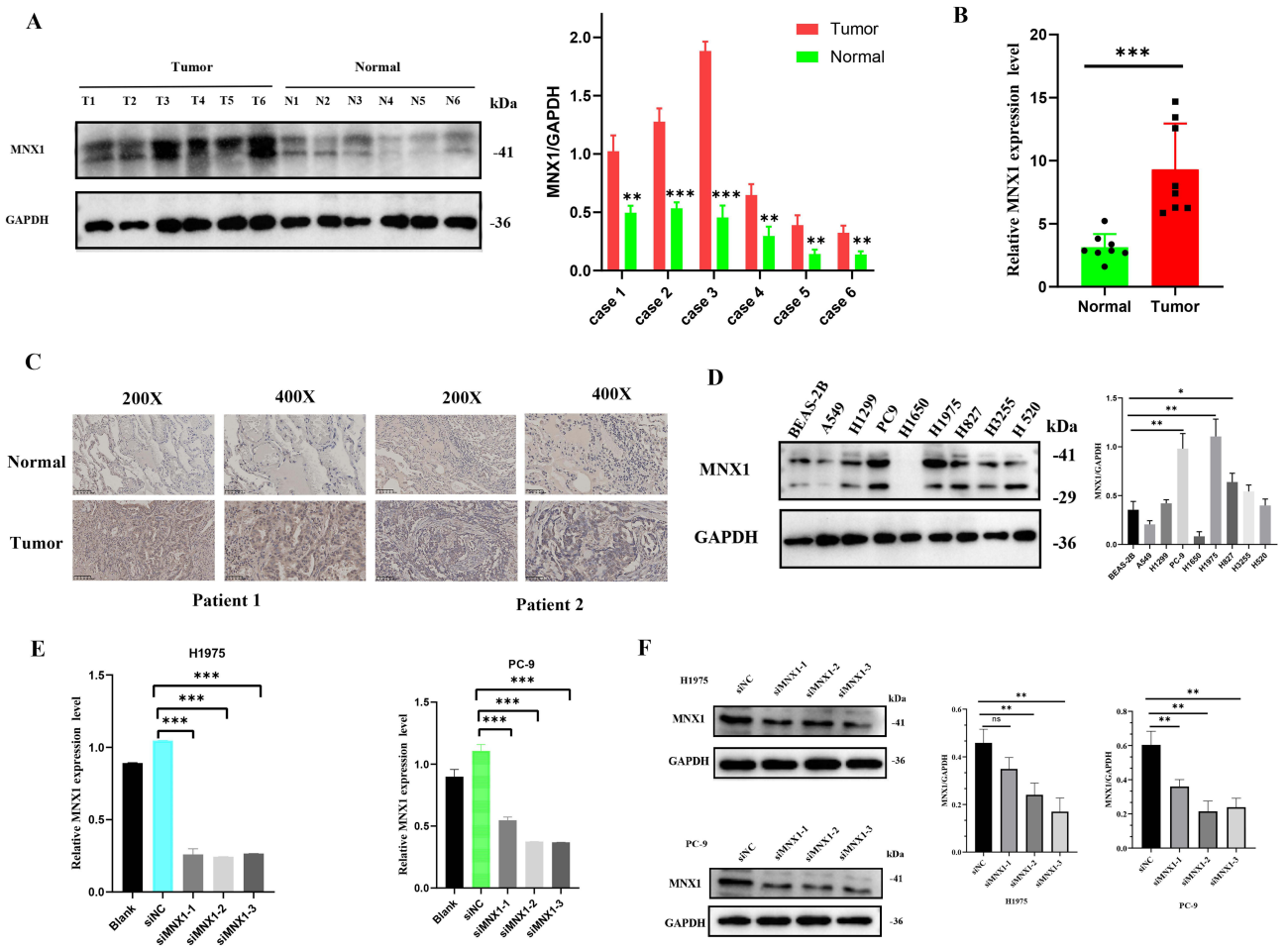

Figure 4 MNX1 is highly expressed in LUAD tumor tissues and cell lines. Postoperative LUAD tumor and paracancerous tissues were obtained, (**A**) Western blot and (**B**) RT-PCR analyses revealed that MNX1 mRNA and protein levels were significantly elevated in tumor tissues compared with paracancerous tissues. (**C**) IHC results revealed that MNX1 was predominantly localized in the nucleus and cytoplasm of LUAD tumor tissue, with significantly higher expression compared with paracancerous tissues. (**D**) Western blot assays demonstrated higher MNX1 protein expression in EGFR mutant LUAD cells (PC-9, H1975, H1299, and H827) than EGFR wildtype cells (A549) and BEAS-2B. (**E**) RT-PCR and (**F**) Western blot analyses confirmed that si-RNA treatment significantly reduced MNX1 expression levels in LUAD cells. IHC, immunohistochemical staining; BEAS-2B, human immortalized lung epithelial cell line. *$P < 0.05$, **$P < 0.01$, ***$P < 0.001$.

identified the PI3K/AKT signaling pathway as potentially significant in LUAD regulation (Figure 8A, and Table 4). When LUAD cells were treated with siMNX1 or osimertinib, Western blot assays demonstrated that MNX1 blockade or osimertinib treatment upregulated E-cadherin while downregulating N-cadherin, vimentin, and the invasion protein MMP9 (Figure 8C and D). Besides, the phosphorylation of EGFR and AKT was reduced (Figure 8E and F), and MNX1 downregulation also suppressed PD-L1 expression (Figure 8E and F). However, non-significant changes were observed in the expression levels of non-phosphorylated EGFR and AKT proteins. Furthermore, co-culture of LUAD cells with siMNX1 and osimertinib reduced EMT markers, MMP9, PD-L1, and EGFR and AKT phosphorylation in PC-9, H1975, and H1975-OR (Figure 8G and H). These findings suggest that abnormally activated MNX1 affects PD-L1 expression and induced EMT, promoting osimertinib resistance via the EGFR signaling axis. As reported in previous studies, EMT and elevated PD-L1 expression are associated with EGFR-TKIs resistance.[23–25]

MNX1 Depletion Inhibits Xenograft Tumor Growth and Reverses Osimertinib Resistance in vivo

To evaluate the effect of silenced MNX1 expression on tumorigenesis and its potentiation of osimertinib in vivo, PC-9 cells were infected with lentiviral stable transfections and divided into four groups: LV-shNC, shMNX1, osimertinib, and shMNX1 + osimertinib. A xenograft mouse model was constructed to establish transplant tumor models in nude mice

https://doi.org/10.2147/DDDT.S535214

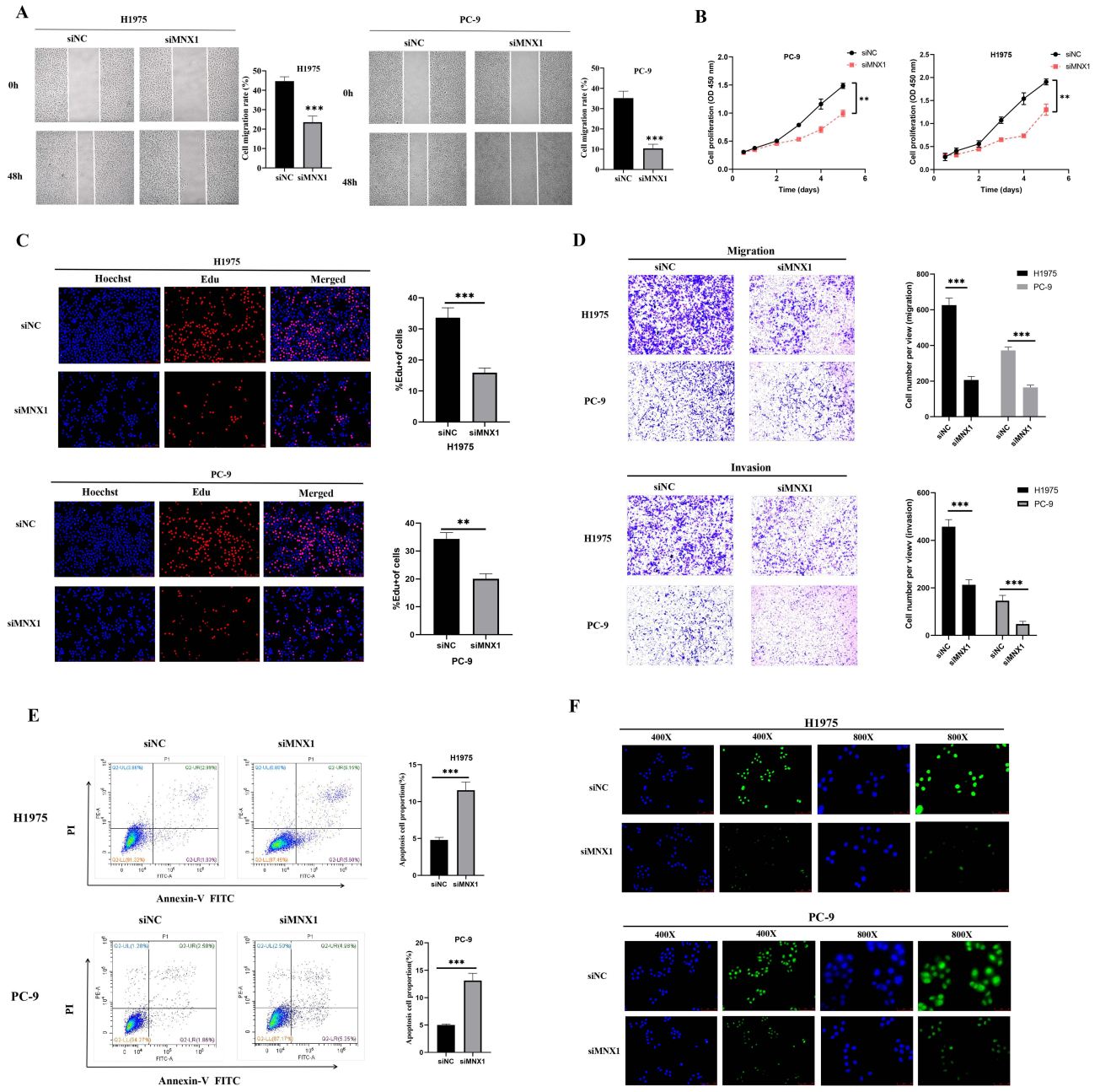

Figure 5 MNX1 positively regulates tumor growth and metastasis in LUAD cells in vitro. (**A**) Wound healing assay demonstrated that suppressed MNX1 expression significantly inhibited the migration capacity of PC-9 and H1975 cells. (**B**) CCK-8 and (**C**) EdU assays (×200 magnification) demonstrated that MNXI promoted the proliferation of PC-9 and H1975 cells. (**D**) Transwell assays revealed that the knockdown of MNX1 expression significantly inhibited the migration and invasion abilities of PC-9 and H1975 cells. (**E**) Flow cytometry analysis revealed that MNX1 knockdown significantly increased the apoptosis rate of LUAD cells. (**F**) Immunofluorescence assays indicated that MNX1 was primarily localized in the nucleus, and downregulation of MNX1 significantly reduced the fluorescent brightness in LUAD cells. $^{**}P < 0.01$, $^{***}P < 0.001$.

(Figure 9A). As depicted in Figure 9B and C, tumor size in the combination shMNX1 and osimertinib group was significantly reduced than the shMNX1 or osimertinib groups during the treatment period. Moreover, RT-PCR indicated that MNX1 expression in the combination group was significantly lower than in either the shMNX1 or osimertinib groups (Figure 9D). Western blot analysis revealed that silencing MNX1 expression significantly enhanced osimertinib sensitivity, upregulated E-cadherin, and downregulated N-cadherin and vimentin (Figure 9E); EGFR and AKT phosphorylation were also decreased (Figure 9F). Immunohistochemical staining further demonstrated a significant reduction in MNX1, Ki-67, N-cadherin, and vimentin expression, alongside an upregulation in E-cadherin, compared with other

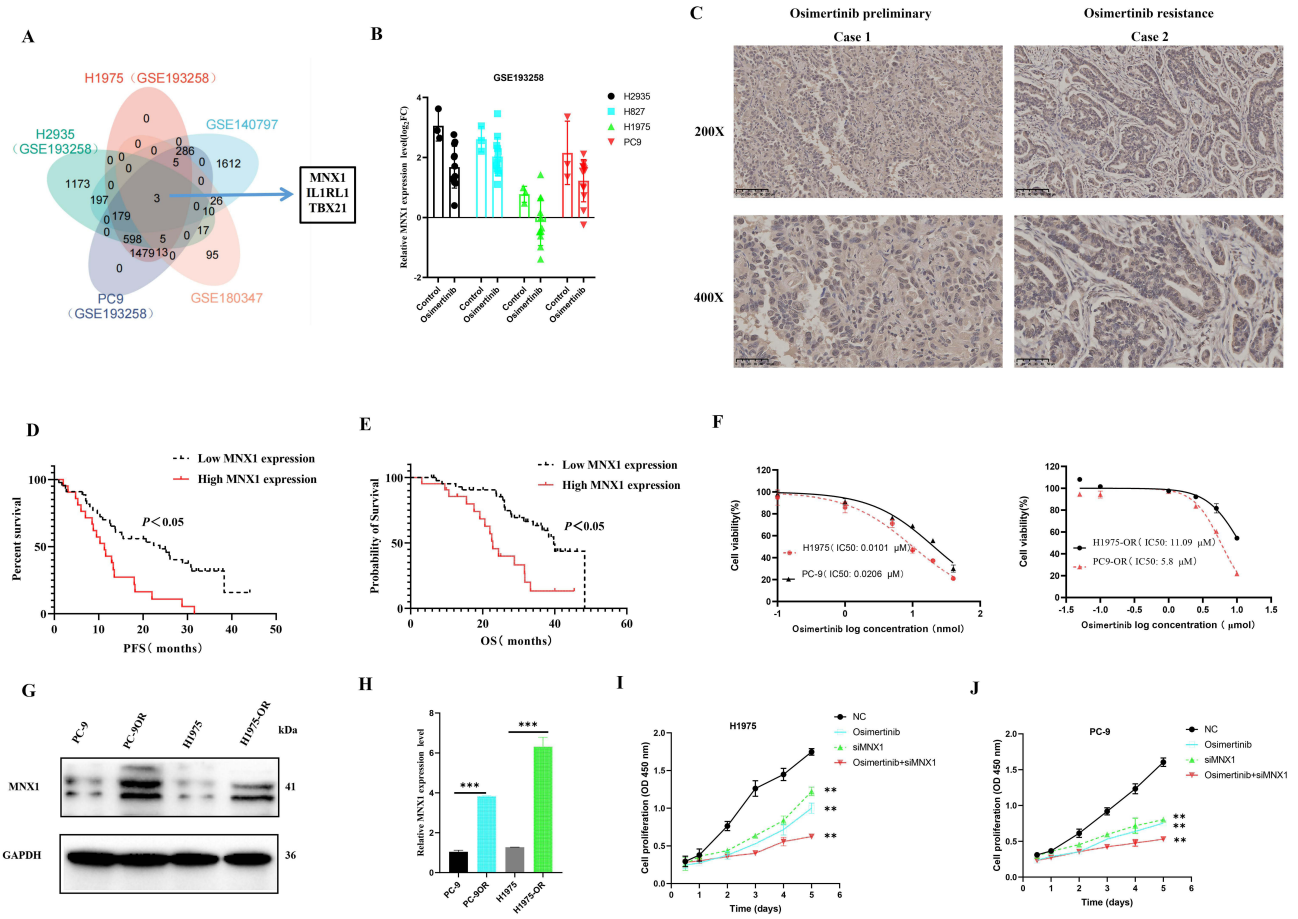

Figure 6 MNX1 contributes to acquired resistance to first-line osimertinib in advanced EGFR-mutant lung cancers. (**A**) Four LUAD cells (H2935, H827, H1975, and PC-9) were treated with osimertinib, and mRNA expression levels were analyzed using a microarray expression profiling dataset downloaded from the GEO database (GSE193258). Venn diagram presented three DEGs overlapping between GSE193258, GSE140797, and GSE180347, with MNX1 being expressed in all three datasets. (**B**) MNX1 expression was lower in osimertinib-treated groups compared with the untreated groups in EGFR-mutant LUAD cells (H2935, H1975, and PC-9) from the GSE193258 database. (**C**) Paraffin-embedded tissues in patients with EGFR-mutant advanced NSCLC treated with osimertinib were collected; IHC revealed that MNX1 expression was higher in the osimertinib-resistant group than in the osimertinib sensitive group, with high MNX1 expression correlating with worse (**D**) PFS and (**E**) OS. (**F**) Osimertinib-sensitive (PC-9 and H1975) and resistant (PC9-OR and H1975-OR) LUAD cells were cultured, and the osimertinib-resistant cells were continuously cultured at low concentration (0.1 μmol/L). The IC_{50} values were tested by CCK-8 assay. (**G**) Western blot and (**H**) RT-PCR illustrated MNX1 overexpression in PC9-OR and H1975-OR than in PC-9 and H1975. When LUAD cells were co-cultured with siMNX1 and osimertinib, the CCK-8 assay demonstrated that this combination significantly inhibited (**I**) H1975 and (**J**) PC-9 cell proliferation. $^{**}P < 0.01$, $^{***}P < 0.001$.

groups (Figure 9G). Taken together, these data suggested that silencing MNX1 expression can inhibit AKT-mediated EMT expression, thereby overcoming osimertinib resistance in LUAD cells in vivo *and vitro* (Figure 9H).

Discussion

Osimertinib, a third-generation EGFR-TKI, significantly prolongs median OS and PFS and serves as a first- or further-line standard treatment for EGFR-mutant advanced NSCLC.[2–4] However, most patients develop drug resistance following oral targeted drug therapy, leading to disease progression. Studies report that approximately 50–70% of osimertinib resistance is associated with primary or secondary resistance, including activation of the HGF/c-MET, RAS-MAPK, and PI3K/AKT pathways.[5–10] Additionally, abnormal activation of cytokines or kinase-activated bypass pathways accounts for 20–30% of osimertinib resistance in EGFR-mutant advanced NSCLC. The EGFR-independent resistance mechanisms remain complex and controversial. Consequently, understanding the mechanisms of osimertinib resistance and generating laboratory data for effective treatment strategies in EGFR-mutant advanced NSCLC is crucial.

Research has demonstrated that abnormally activated mRNA can serve as a key biomarker for tumor progression and drug resistance. Fibrinogen-like protein 1 (FGL1) is highly expressed in NSCLC tissues, with low FGL1 expression

https://doi.org/10.2147/DDDT.S535214

Table 3 Univariate Logistic Analysis MNX1 Expression and Clinicopathological Features by IHC in NSCLC

Characteristic		MNX1 (n=65)		OR (95% CI)	*P value*
		Low Expression	High Expression		
Gender	Male	19	7	Ref	
	Female	25	14	1.52(0.513–4.502)	0.45
Age(years)	≤60	21	10	Ref	
	>60	23	11	1.004(0.355–2.844)	0.993
ECOG PS	0-1	37	15	Ref	
	2	7	6	1.454(0.78–2.709)	0.238
Smoking	No	38	18	Ref	
	Yes	6	3	1.056(0.237–4.707)	0.943
T **stage**	T1	14	6	Ref	0.184
	T2	16	3	0.438(0.092–2.083)	0.299
	T3	8	4	1.167(0.251–5.413)	0.844
	T4	7	7	2.722(0.638–11.61)	0.176
N **stage**	N0	8	3	Ref	0.721
	N1	4	0	-	0.999
	N2	26	11	1.128(0.251–5.069)	0.875
	N3	7	6	2.286(0.41–12.732)	0.345
TNM stage	II–III	10	0	Ref	
	IV	34	21		
Brain metastasis	Non-metastasis	29	11	Ref	
	Metastasis	15	10	1.758(0.609–5.069)	0.297
CEA (ng/mL)[a]	≤6.5	12	6	Ref	
	>6.5	32	15	0.938(0.295–2.979)	0.913
EGFR mutation	Del 19	27	11	Ref	
	L858R	17	10	1.444(0.505–4.124)	0.493
TP53	Wild-type	23	10	Ref	
	Mutant-type	21	11	1.205(0.425–3.411)	0.726
Cyfra211(ng/mL)[a]	≤3.3	25	4	Ref	
	>3.3	19	17	5.592(1.615–19.36)	0.007
NSE (ng/mL) [a]	≤16.3	25	7	Ref	
	>16.3	19	14	2.632(0.888–7.794)	0.081

Note: [a]The cut-off points was used relevant assay kits.
Abbreviations: ECOG PS, Eastern Cooperative Oncology Group performance status; CEA, carcinoembryonic antigen; Cyfra211, cytokeratin 19 fragment; NSE, neural specific enolase.

associated with improved therapeutic responses, making it a predictive biomarker for therapeutic efficacy in NSCLC.[26] Similarly, YKT6 is associated with clinical characteristics such as staging, smoking, lymph node metastasis, and TP53 mutation; its high expression is associated with poor prognosis, identifying it as a new biomarker for LUAD diagnosis and prognosis.[27] In this study, we analyzed seven pairs of LUAD tumor and paracancerous tissues from GEO databases, identifying 44 DEGs associated with LUAD. Furthermore, RT-PCR demonstrated that MNX1 expression was elevated in LUAD tumor tissues and cells compared with normal tissues and BEAS-2B cells, correlating with poor prognosis. The ROC curve analysis using TCGA data demonstrated that MNX1 possesses high specificity and sensitivity for diagnosing LUAD, indicating its role as a significant oncogene. Consequently, MNX1 may serve as a key biomarker for LUAD, warranting further investigation.

The study discovered that MNX1 is vital for motor neuron differentiation, pancreatic β-cell development, and nuclear division regulation.[16] As a tumor promoter, MNX1 is highly expressed in tumor tissues compared with normal tissues, correlating with poor prognosis in breast cancer. Pathway enrichment analysis further revealed that MNX1 regulates nuclear division, cell cycle, and p53 signaling processes.[17] Moreover, MNX1 upregulates c-MYC and CCND1

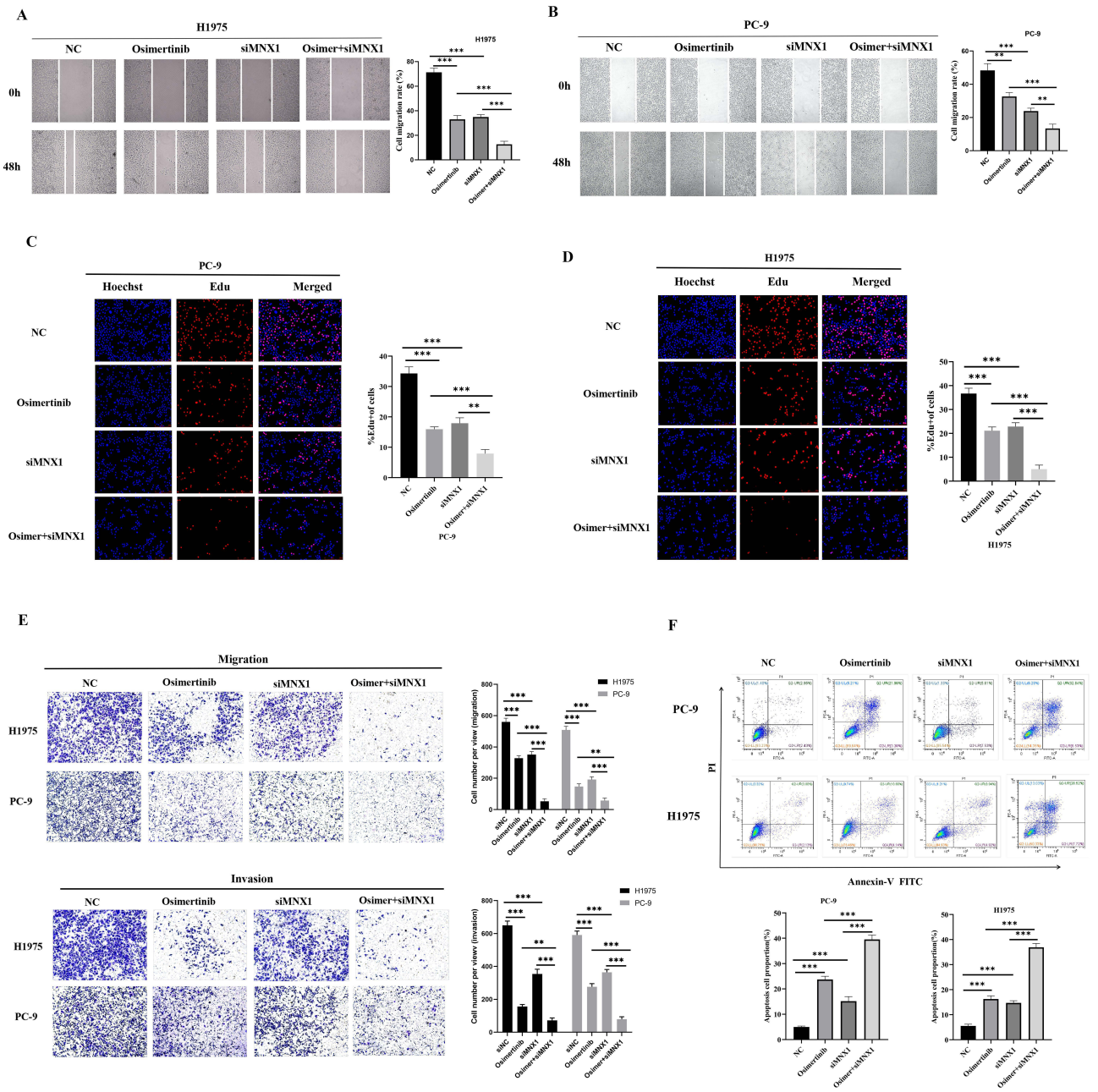

Figure 7 MNX1 blockade potentiated osimertinib to suppress LUAD cells growth and proliferation. The LUAD cells were con-cultured with siMNX1 and Osimertinib, the cell wound healing assay is used to evaluate cell mobility by measuring the scratch width under a microscope in (**A**) H1975 and (**B**) PC-9. The EdU assay is used to evaluate the cell proliferation ability in (**C**) PC-9 and (**D**) H1975. (**E**) Transwell assays assay is used to evaluate the proliferation and invasion capacity of PC-9 and H1975 cells. (**F**) The flow cytometric assays showed that the apoptosis rate of LUAD cells were significantly increased in the combination of group. $^{**}P < 0.01$, $^{***}P < 0.001$.

expression, promoting CRC cell distant metastasis and proliferation through Wnt/β- catenin signaling pathway.[18] MNX1 overexpression unregulated SREBP1 expression and fatty acid synthetase, potentially promoting lipid synthesis in prostate cancer.[20] Melo et al analyzed the relationship between genetic variants and normal lung development, revealing that MACS1 enhancer inappropriate activation elevates MNX1 expression, which contributes to lung malformations, including lung agenesis.[28] However, the role of MNX1 in proliferation and its prognostic value in LUAD remains underexplored. In this study, multivariable COX analysis identified MNX1, combined with clinicopathological factors, as an independent prognostic factor for OS in LUAD. Nomogram and calibration plots demonstrated that MNX1, combined with clinical factors, could predict 1-, 2-, and 3-year OS probabilities in LUAD. The RT-PCR results revealed that MNX1

https://doi.org/10.2147/DDDT.S535214

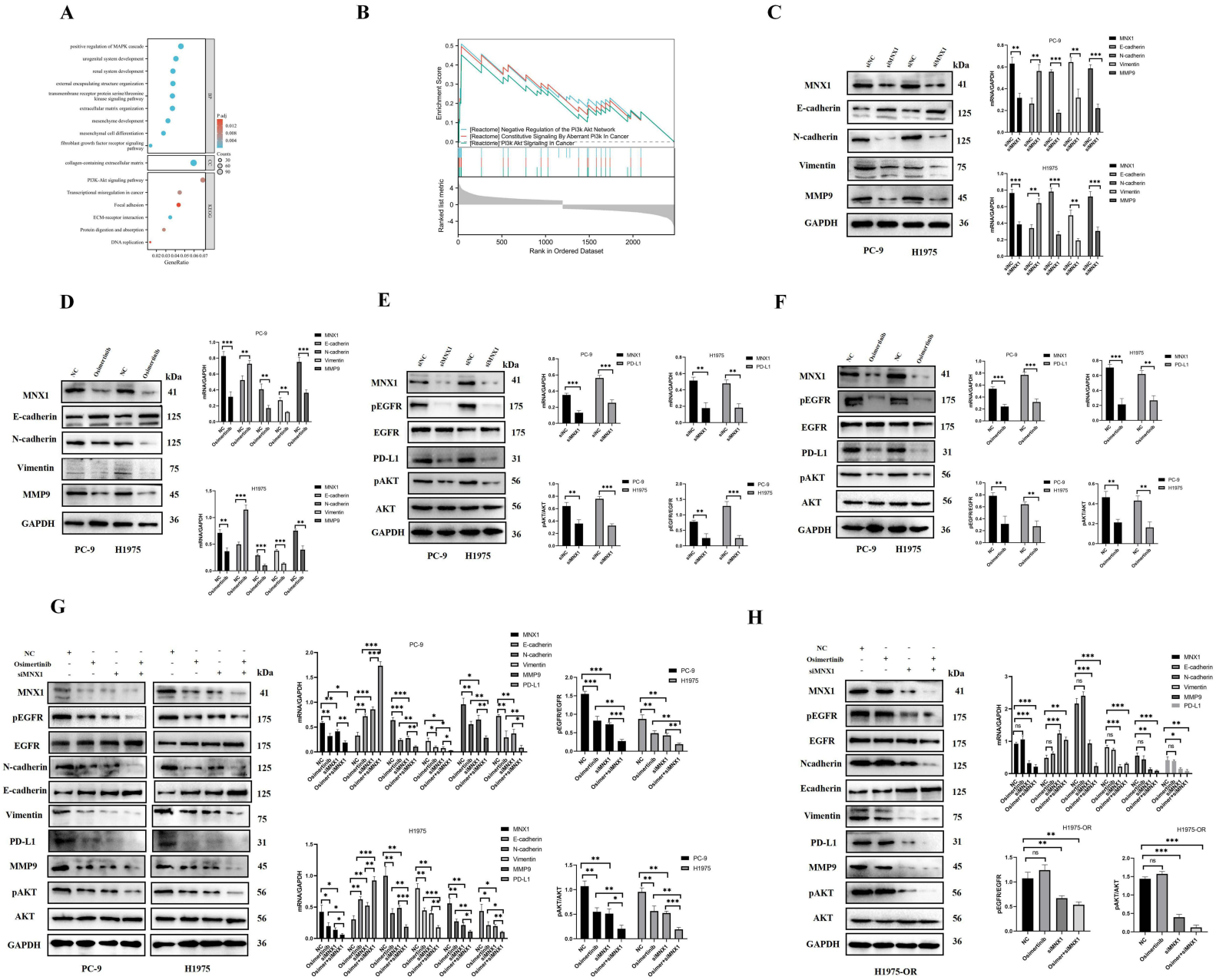

Figure 8 Abnormally activated MNX1 affected PD-L1 expression and induced to reverse osimertinib resistance in LUAD cells via the EGFR signaling pathway. DEGs in patients with LUAD and cells from the GSE140797 and GSE193258 databases were analyzed. (**A**) KEGG/GO and (**B**) GSEA pathway enrichment analyses identified the PI3K/AKT signaling pathway as potentially crucial in regulating LUAD. (**C**) The LUAD cells cultured with siMNX1, Western blot assays was performed to detect the EMT-related protein. (**D**) Western blot assays was performed to detect the EMT-related protein following the LUAD cells cultured with osimertinib. (**E**) Western blot assays analysis of EGFR, pEGFR, PD-L1, pAKT and AKT expression after MNX1 downregulation. (**F**) Western blot assays analysis of EGFR, pEGFR, PD-L1, pAKT and AKT expression after cultured with osimertinib. (**G**) Western blot assays analysis of EMT-related protein, EGFR, pEGFR, PD-L1, MMP9, pAKT and AKT expression after PC-9 and H1975 cells were co-cultured with siMNX1 and osimertinib. (**H**) Western blot assays analysis of EMT-related protein, EGFR, pEGFR, PD-L1, MMP9, pAKT and AKT expression after H1975-OR cells were co-cultured with siMNX1 and osimertinib. *$P < 0.05$, **$P < 0.01$, ***$P < 0.001$.

Abbreviations: LUAD, lung adenocarcinoma; EMT, epithelial-mesenchymal transition; H1975-OR, osimertinib-resistant lung adenocarcinoma cells.

Table 4 The Correlation MNX1 Relate Differential Expression Genes with Signaling Pathway From KEGG Database in LUAD Patients

ONTOLOGY	ID	Description	GeneRatio	BgRatio	*P* value	*P*.adjust	Count
GO	GO:0001655	Urogenital system development	77/1892	352/18,800	< 0.001	< 0.001	77
GO	GO:0030198	Extracellular matrix organization	70/1892	307/18,800	< 0.001	< 0.001	70
GO	GO:0072001	Renal system development	71/1892	312/18,800	< 0.001	< 0.001	71
GO	GO:0043062	Extracellular structure organization	70/1892	308/18,800	< 0.001	< 0.001	70
GO	GO:0060485	Mesenchyme development	61/1892	301/18,800	< 0.001	< 0.001	61
GO	GO:0043410	Positive regulation of MAPK cascade	87/1892	491/18,800	< 0.001	< 0.001	87
GO	GO:0007178	Transmembrane receptor protein serine/threonine kinase signaling pathway	70/1892	368/18,800	< 0.001	< 0.001	70
GO	GO:0008543	Fibroblast growth factor receptor signaling pathway	26/1892	85/18,800	< 0.001	< 0.001	26
GO	GO:0010975	Regulation of neuron projection development	78/1892	431/18,800	< 0.001	< 0.001	78
GO	GO:0051960	Regulation of nervous system development	79/1892	440/18,800	< 0.001	< 0.001	79
GO	GO:0070371	ERK1 and ERK2 cascade	64/1892	335/18,800	< 0.001	< 0.001	64
GO	GO:0070372	Regulation of ERK1 and ERK2 cascade	57/1892	311/18,800	< 0.001	< 0.001	57
GO	GO:0030324	Lung development	38/1892	179/18,800	< 0.001	< 0.001	38
GO	GO:0001837	Epithelial to mesenchymal transition	33/1892	162/18,800	< 0.001	0.0021	33
GO	GO:0030509	BMP signaling pathway	33/1892	162/18,800	< 0.001	0.0021	33
GO	GO:0043405	Regulation of MAP kinase activity	36/1892	183/18,800	< 0.001	0.0021	36
GO	GO:0070374	Positive regulation of ERK1 and ERK2 cascade	40/1892	220/18,800	< 0.001	0.0043	40
KEGG	hsa04512	ECM-receptor interaction	31/895	88/8164	< 0.001	< 0.001	31
KEGG	hsa05202	Transcriptional misregulation in cancer	40/895	193/8164	< 0.001	0.0075	40
KEGG	hsa04974	Protein digestion and absorption	25/895	103/8164	< 0.001	0.0085	25
KEGG	hsa04151	PI3K-Akt signaling pathway	62/895	354/8164	< 0.001	0.0085	62
KEGG	hsa04510	Focal adhesion	39/895	201/8164	< 0.001	0.0156	39
KEGG	hsa03030	DNA replication	12/895	36/8164	< 0.001	0.0156	12
KEGG	hsa05222	Small cell lung cancer	20/895	92/8164	0.0019	0.0422	20

expression was higher in EGFR mutant LUAD cells compared with EGFR wildtype A549 cells. Elevated MNX1 expression promoted LUAD cell proliferation and metastasis while inhibiting apoptosis in vitro. These findings as the study have reported that MNX1 acts as an oncogene, directly binding to the CCDC34 promoter to activate its expression, thereby enhancing LUAD cell proliferation and growth.[21]

Previous studies have identified abnormal activation of cytokines or kinase-activated bypass pathways as contributors to osimertinib resistance in EGFR-mutant advanced NSCLC. For instance, abnormally activated ID1 mediates osimertinib resistance in EGFR T790M-positive NSCLC through EMT.[15] Besides, the MERTK ligand GAS6 activates downstream oncogenic signaling, further promoting osimertinib resistance in LUAD cells.[29] Estrogen receptor β (ERβ) has been reported to be significantly expressed in NSCLC resistant to osimertinib, playing a crucial role in fostering resistance to the drug; Erβ stabilization by USP7 reduces PRDX3 SUMOylation, lowering ROS accumulation and enhancing resistance to osimertinib.[30] Yi et al identified HER3 as an upstream regulator of PAK2/β-catenin signaling, which promotes the acquisition of osimertinib resistance in EGFR-mutant LUAD cells.[31] However, the molecular mechanisms of MNX1 and its role in promoting osimertinib resistance remain controversial and warrant further investigation.

In this study, MNX1 was more highly expressed in EGFR-mutant LUAD cells than EGFR wildtype. DEGs analysis from the GEO database revealed lower MNX1 expression in osimertinib-treated groups than in untreated groups of EGFR-mutant LUAD cells, suggesting that MNX1 acts as an oncogene and may contribute to osimertinib resistance. Paraffin-embedded tissues were collected and analyzed using IHC. Results indicated that MNX1 expression was higher in patients with osimertinib-resistance than patients with osimertinib-sensitivity, with elevated MNX1 levels associated with worse mPFS. Osimertinib-sensitive and resistant LUAD cells were cultured, with osimertinib-resistant cells continuously cultured at low concentrations. Cell assays demonstrated that MNX1 blockade enhanced the ability of osimertinib to suppress LUAD cell growth and proliferation. Western blot analysis demonstrated that MNX1 blockade upregulated E-cadherin, downregulated N-cadherin and vimentin, and inhibited the invasion protein of MMP9. These findings suggest that abnormally activated MNX1 promotes osimertinib resistance through EMT in EGFR-mutant LUAD cells.

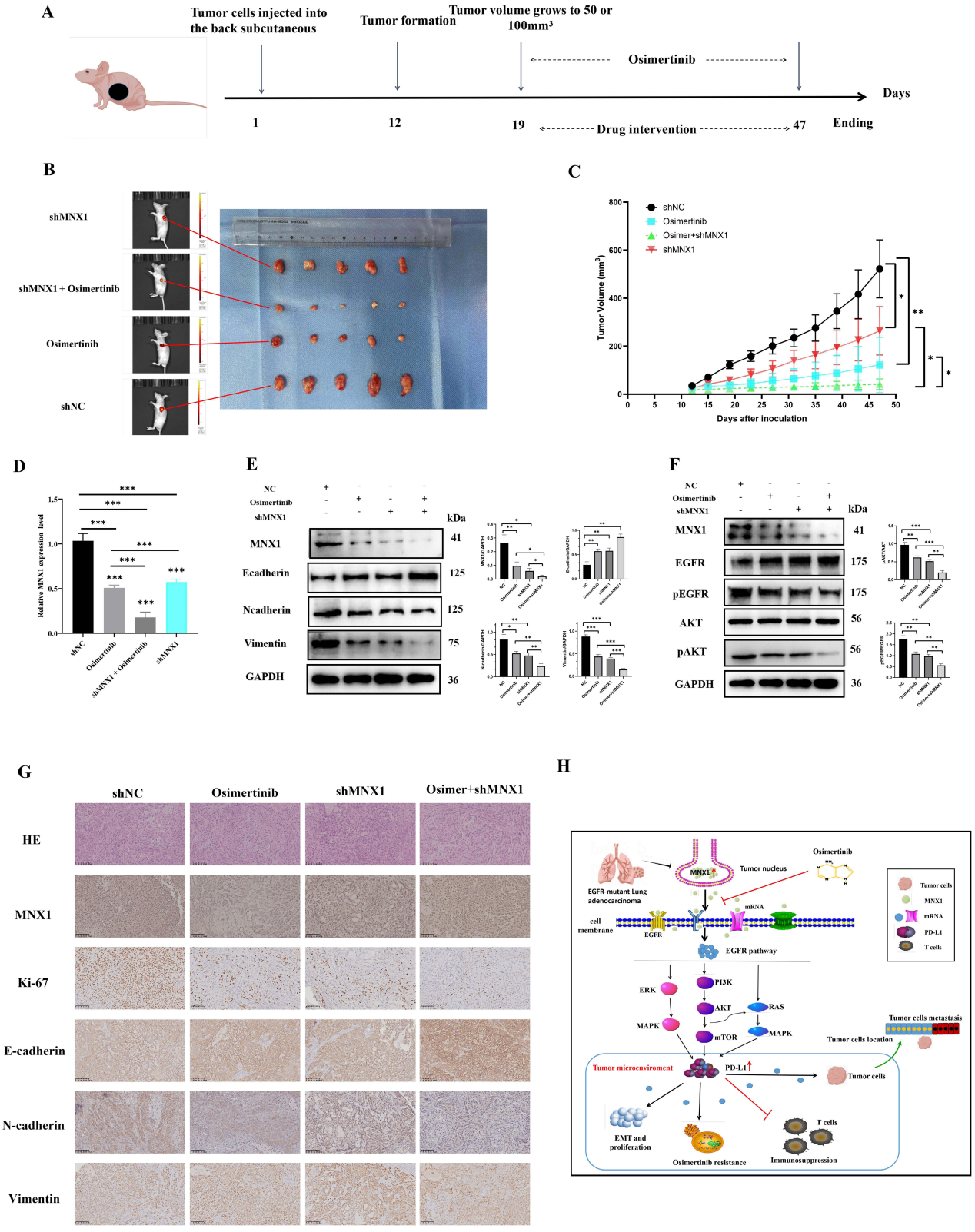

Figure 9 MNX1 depletion inhibits xenograft tumor growth and reverses osimertinib resistance in vivo. (**A**) PC-9 cells were infected with lentiviral stable transfections and categorized into LV-shNC, PC-9^{MNX1+}, osimertinib, and PC-9^{MNX1+} + osimertinib groups to construct a xenograft mouse model and establish tumor models in nude mice. (**B**) Tumor tissues were harvested after 47 days. (**C**) The tumor volume was measured using calipers and calculated with the formula. (**D**) The MNX1 expression were detected by RT-PCR. (**E**) Western blot assays analysis of EMT-related protein. (**F**) Western blot assays analysis of EGFR, pEGFR, pAKT and AKT expression. (**G**) Tumor tissues from nude mice were embedded in paraffin, the MNX1, Ki-67, EMT-related protein levels were detected by IHC. (**H**) The proposed working model of that abnormally activated MNX1 affects PD-L1 expression and promoted EMT, contributing to osimertinib resistance in LUAD cells through the EGFR signaling pathway. *P < 0.05, **P < 0.01, ***P < 0.001.

Numerous studies have linked osimertinib resistance to HGF/c-MET, RAS-MAPK, and PI3K/AKT pathways activation.[7–10] Tian et al reported that osimertinib-resistant cells induced MEK1 and AKT1/2 activation, weakening osimertinib sensitivity. Bypass or downstream activation represents an important mechanism for drug resistance.[14] Additionally, SOS2 overexpression facilitated EMT, reactivated RTK/AKT signaling, and enhanced osimertinib resistance in LUAD cells, underscoring the pivotal role of EGFR in signaling osimertinib efficacy and resistance.[32] In this study, related DEGs in patients with LUAD and cells were analyzed using the GEO database, with KEGG/GO and GSEA pathway enrichment analyses identifying the PI3K/AKT signaling pathway as a key regulator in LUAD. Furthermore, MNX1 was observed to correlate with the immune microenvironment. When LUAD cells were cultured with siMNX1 or osimertinib, phosphorylation of EGFR and AKT proteins was significantly inhibited, along with suppression of PD-L1 expression. Furthermore, co-treatment of LUAD cells with siMNX1 and osimertinib led to a greater reduction in PD-L1 expression and phosphorylation of EGFR and AKT. These findings suggest that abnormally activated MNX1 affects PD-L1 expression and promotes EMT, thereby driving osimertinib resistance through the EGFR signaling axis. This aligns with previous studies indicating that EMT and elevated PD-L1 expression contribute to EGFR-TKI resistance.[23–25]

Despite the significant insights provided by this study, several limitations should be acknowledged. First, although we have identified the role of MNX1 in mediating osimertinib resistance in EGFR-mutant LUAD, the complexity of bypass signaling pathways remains incompletely understood. There are likely other key molecules and pathways involved in this process that were not explored in our current research. Second, our study was mainly based on in- vitro cell line experiments and in-vivo xenograft mouse models. The cell lines used, such as the PC9 cell line with its specific EGFR mutation (L858R/T790M), may not fully represent the heterogeneity of EGFR-mutant LUAD in clinical settings. Different patients' tumors may have diverse genetic backgrounds, epigenetic modifications, and tumor microenvironments that could affect the role of MNX1 and the development of osimertinib resistance. Third, in terms of clinical translation, although we have proposed MNX1 as a potential prognostic biomarker and therapeutic target, further large-scale clinical trials are needed to validate our findings. To establish MNX1 as a reliable biomarker in the clinic, a much larger cohort of patients with EGFR-mutant LUAD, preferably from different ethnic groups and with diverse treatment histories, should be examined. Additionally, we did not analysis of the relationship between MNX1 and MET amplification, HER2 activation, KRAS mutation etc, it is unclear whether MNX1 operates independently or synergistically with canonical resistance pathways. Fourth, our understanding of the molecular mechanisms underlying the regulation of MNX1 in LUAD is still in its infancy. While we have demonstrated that abnormally activated MNX1 promotes LUAD cell growth and osimertinib resistance through AKT-mediated EMT and PD-L1 upregulation, the upstream regulators of MNX1 and the precise epigenetic and transcriptional mechanisms controlling its expression are yet to be fully elucidated. Moreover, further research is needed to clarify the mechanisms of tumor cell immune escape caused by EGFR-TKI resistance and provide additional laboratory data supporting the use of combined TKIs and immunotherapy strategies.

Conclusions

In summary, our findings suggest that MNX1 is a tumorigenic factor associated with poor prognosis and high diagnostic specificity and sensitivity in LUAD. MNX1 overexpression promotes proliferation and metastasis while inhibiting apoptosis in LUAD cells. Additionally, MNX1 was highly expressed in EGFR-mutant and osimertinib-resistant LUAD cells. Cell assays confirmed that MNX1 blockade enhanced the effectiveness of osimertinib in suppressing LUAD cell growth and proliferation in vitro and in vivo. We propose that abnormally activated MNX1 contributes to osimertinib resistance by promoting AKT-mediated EMT and PD-L1 expression, thereby facilitating LUAD cell growth and proliferation. As a promising prognostic biomarker and therapeutic target, MNX1 can help overcome osimertinib resistance in EGFR-mutant advanced LUAD.

Date Availability Statement

The data generated and analyzed during the current study are available from the Weiguo Gu for data sharing on reasonable request.

Ethical Approval

This study, including the use of cell lines, has been reviewed and approved by the ethics institution committee of The First Affiliated Hospital, Jiangxi Medical College, Nanchang University (No. (2024)CDYFYYLK(08-012)). Our study of ethics are also according with the declaration of Helsinki. Written informed consent was obtained from all participants or their legal guardians prior to sample collection. All animal experiments were approved by the Medical Ethics Committee of First Affiliated Hospital of Nanchang University (No. CDYFY-IACUC-202304QR025) and conducted according to the Guidelines for the Care and Use of Animals for Scientific Research.

Author Contributions

All authors made a significant contribution to the work reported, whether that is in the conception, study design, execution, acquisition of data, analysis and interpretation, or in all these areas; took part in drafting, revising or critically reviewing the article; gave final approval of the version to be published; have agreed on the journal to which the article has been submitted; and agree to be accountable for all aspects of the work.

Funding

This work was supported by Jiangxi Provincial Natural Science Foundation (No.20232BAB216086), Jiangxi Provincial Chinese Medicine Science (No.2023B0049) and Nanchang University (No.ZL094), Jiangxi Provincial Key R&DPlan "Unveiling the List and Taking Command"Project(20223BBH80009).

Disclosure

The authors declare that they have no competing interests in this work.

References

1. Sung H, Ferlay J, Siegel RL, et al. Global cancer statistics 2020: GLOBOCAN estimates of incidence and mortality worldwide for 36 cancers in 185 countries. *CA Cancer J Clin*. 2021;71(3):209–249. doi:10.3322/caac.21660
2. Soria JC, Ohe Y, Vansteenkiste J, et al. Osimertinib in untreated EGFR-mutated advanced non-small-cell lung cancer. *N Engl J Med*. 2018;378(2):113–125. doi:10.1056/NEJMoa1713137
3. Rosell R, Carcereny E, Gervais R, et al. Erlotinib versus standard chemotherapy as first-line treatment for European patients with advanced EGFR mutation-positive non-small-cell lung cancer (EURTAC): a multicentre, open-label, randomised phase 3 trial. *Lancet Oncol*. 2012;13(3):239–246. doi:10.1016/S1470-2045(11)70393-X
4. Mok TS, Wu Y-L, Ahn M-J, et al. Osimertinib or platinum-pemetrexed in EGFR T790M-positive lung cancer. *N Engl J Med*. 2017;376(7):629–640. doi:10.1056/NEJMoa1612674
5. Remon J, Moran T, Majem M, et al. Acquired resistance to epidermal growth factor receptor tyrosine kinase inhibitors in EGFR-mutant non-small cell lung cancer: a new era begins. *Cancer Treat Rev*. 2014;40(1):93–101. doi:10.1016/j.ctrv.2013.06.002
6. Fu K, Xie F, Wang F, Fu L. Therapeutic strategies for EGFR-mutated non-small cell lung cancer patients with osimertinib resistance. *J Hematol Oncol*. 2022;15(1):173. doi:10.1186/s13045-022-01391-4
7. Gadgeel SM, Wozniak A. Preclinical rationale for PI3K/Akt/mTOR pathway inhibitors as therapy for epidermal growth factor receptor inhibitor-resistant non-small-cell lung cancer. *Clin Lung Cancer*. 2013;14(4):322–332. doi:10.1016/j.cllc.2012.12.001
8. Zhou B, Tang C, Li J. K-RAS mutation and resistance to epidermal growth factor receptor-tyrosine kinase inhibitor treatment in patients with non-small cell lung cancer. *J Can Res Ther*. 2017;13(4):699–701. doi:10.4103/jcrt.JCRT_468_17
9. Shi P, Oh YT, Zhang G, et al. MET gene amplification and pro-tein hyperactivation is a mechanism of resistance to both first and third generation EGFR inhibitors in lung cancer treatment. *Cancer Lett*. 2016;380(2):494–504. doi:10.1016/j.canlet.2016.07.021
10. Yi Y, Zeng S, Wang Z, et al. Cancer-associated fibroblasts promote epithelial-mesenchymal transition and EGFR-TKI resistance of non-small cell lung cancers via HGF/IGF-1/ANXA2 signaling. *Biochim Biophys Acta Mol Basis Dis*. 2018;1864(3):793–803. doi:10.1016/j.bbadis.2017.12.021
11. Tamura T, Kato Y, Ohashi K, et al. Potential influence of interleukin-6 on the therapeutic effect of gefitinib in patients with advanced non-small cell lung cancer harbouring EGFR mutations. *Biochem Biophys Res Commun*. 2018;495(1):360–367. doi:10.1016/j.bbrc.2017.10.175
12. Kim SM, Kwon OJ, Hong YK, et al. Activation of IL-6R/JAK1/STAT3 signaling induces de novo resistance to irreversible EGFR inhibitors in non-small cell lung cancer with T790M resistance mutation. *Mol Cancer Ther*. 2012;11(10):2254–2264. doi:10.1158/1535-7163.MCT-12-0311
13. Chen SF, Zhang ZY, Zhang JL. Matrine increases the inhibitory effects of Afatinib on H1975 cells via the IL-6/JAK1/STAT3 signaling pathway. *Mol Med Rep*. 2017;16(3):2733–2739. doi:10.3892/mmr.2017.6865
14. Tian X, Wang R, Gu T, et al. Costunolide is a dual inhibitor of MEK1 and AKT1/2 that overcomes osimertinib resistance in lung cancer. *Mol Cancer*. 2022;21(1):193. doi:10.1186/s12943-022-01662-1
15. Liu K, Chen X, Wu L, et al. ID1 mediates resistance to osimertinib in EGFR T790M-positive non-small cell lung cancer through epithelial-mesenchymal transition. *BMC Pulm Med*. 2021;21(1):163. doi:10.1186/s12890-021-01540-4
16. Vult von Steyern F, Martinov V, Rabben I, Njå A, de Lapeyrière O, Lømo T. The homeodomain transcription factors Islet 1 and HB9 are expressed in adult alpha and gamma motoneurons identified by selective retrograde tracing. *Eur J Neurosci*. 1999;11(6):2093–2102. doi:10.1046/j.1460-9568.1999.00631.x

17. Tian T, Wang M, Zhu Y, et al. Expression, clinical significance, and functional prediction of MNX1 in breast cancer. *Mol Ther Nucleic Acids*. 2018;13:399–406. doi:10.1016/j.omtn.2018.09.014
18. Yang X, Pan Q, Lu Y, Jiang X, Zhang S, Wu J. MNX1 promotes cell proliferation and activates Wnt/β-catenin signaling in colorectal cancer. *Cell Biol Int*. 2019;43(4):402–408. doi:10.1002/cbin.11096
19. Zhu B, Wu Y, Luo J, et al. MNX1 promotes malignant progression of cervical cancer via repressing the transcription of p21cip1. *Front Oncol*. 2020;10:1307. doi:10.3389/fonc.2020.01307
20. Zhang L, Wang J, Wang Y, et al. MNX1 is oncogenically upregulated in african-american prostate cancer. *Cancer Res*. 2016;76(21):6290–6298. doi:10.1158/0008-5472.CAN-16-0087
21. Wu J, Yue C, Xu W, Li H, Zhu J, Li L. MNX1 facilitates the malignant progress of lung adenocarcinoma through transcriptionally upregulating CCDC34. *Oncol Lett*. 2023;26(2):325. doi:10.3892/ol.2023.13911
22. Liang W, Zhang L, Jiang G, et al. Development and validation of a nomogram for predicting survival in patients with resected non-small-cell lung cancer. *J Clin Oncol*. 2015;33(8):861–869. doi:10.1200/JCO.2014.56.6661
23. Jiang Y, Zhuo X, Wu Y, Fu X, Mao C. PAR2 blockade reverses osimertinib resistance in non-small-cell lung cancer cells via attenuating ERK-mediated EMT and PD-L1 expression. *Biochim Biophys Acta Mol Cell Res*. 2022;1869(1):119144. doi:10.1016/j.bbamcr.2021.119144
24. Peng S, Wang R, Zhang X, et al. EGFR-TKI resistance promotes immune escape in lung cancer via increased PD-L1 expression. *Mol Cancer*. 2019;18(1):165. doi:10.1186/s12943-019-1073-4
25. Isomoto K, Haratani K, Hayashi H, et al. Impact of EGFR-TKI treatment on the tumor immune microenvironment in EGFR mutation-positive non-small cell lung cancer. *Clin Cancer Res*. 2020;26(8):2037–2046. doi:10.1158/1078-0432.CCR-19-2027
26. Liu TY, Yan JS, Li X, et al. FGL1: a novel biomarker and target for non-small cell lung cancer, promoting tumor progression and metastasis through KDM4A/STAT3 transcription mechanism. *J Exp Clin Cancer Res*. 2024;43(1):213. doi:10.1186/s13046-024-03140-6
27. Zhang L, Wang S, Wang L. Comprehensive analysis identifies YKT6 as a potential prognostic and diagnostic biomarker in lung adenocarcinoma. *BMC Cancer*. 2024;24(1):1235. doi:10.1186/s12885-024-12975-3
28. Melo US, Piard J, Fischer-Zirnsak B, et al. Complete lung agenesis caused by complex genomic rearrangements with neo-TAD formation at the SHH locus. *Hum Genet*. 2021;140(10):1459–1469. doi:10.1007/s00439-021-02344-6
29. Yan D, Huelse JM, Kireev D, et al. MERTK activation drives osimertinib resistance in EGFR-mutant non-small cell lung cancer. *J Clin Invest*. 2022;132(15):e150517. doi:10.1172/JCI150517
30. Meng Y, Lin W, Wang N, et al. USP7-mediated ERβ stabilization mitigates ROS accumulation and promotes osimertinib resistance by suppressing PRDX3 SUMOylation in non-small cell lung carcinoma. *Cancer Lett*. 2024;582:216587. doi:10.1016/j.canlet.2023.216587
31. Yi Y, Li P, Huang Y, et al. P21-activated kinase 2-mediated β-catenin signaling promotes cancer stemness and osimertinib resistance in EGFR-mutant non-small-cell lung cancer. *Oncogene*. 2022;41(37):4318–4329. doi:10.1038/s41388-022-02438-z
32. Theard PL, Linke AJ, Sealover NE, et al. SOS2 modulates the threshold of EGFR signaling to regulate osimertinib efficacy and resistance in lung adenocarcinoma. *Mol Oncol*. 2024;18(3):641–661. doi:10.1002/1878-0261.13564